

# The Role of Agmatine in Modulating Autophagy Under Neuroinflammatory Conditions Induced by Metabolic Alteration in Mouse Brain

Ji Young Chang<sup>1,2</sup>, Jiwon Kim<sup>1,2</sup>, Jong Youl Kim<sup>3</sup> and Jong Eun Lee<sup>1,2,4\*</sup>

<sup>1</sup>Department of Anatomy, Yonsei University College of Medicine, Seoul 03722,

<sup>2</sup>Graduate School of Medical Science, Brain Korea 21 Project, Yonsei University College of Medicine, Seoul 03722,

<sup>3</sup>Department of Anatomy, Catholic Kwandong University College of Medicine, Gangneung 25601,

<sup>4</sup>Brain Research Institute, Yonsei University College of Medicine, Seoul 03722, Korea

Changes in microglia, a specialized population of glial cells found in the central nervous system (CNS), is often associated with hyperglycemic conditions. It has been reported that exogenous administration of agmatine (agm) has neuroprotective effects in CNS injuries, including neurodegenerative diseases, while also being involved with modulating macrophage subdivision. In this study, the effects of agmatine on microglial polarization has been investigated and whether this effect can be related to the modulation of autophagy in neuroinflammatory conditions induced by high glucose (HG) concentrations. Neuroinflammatory conditions were mimicked through treatment to BV2 microglial cells. BV2 cells were mainly induced into proinflammatory M1 phenotype when treated with HG (100 mM), shown by the increase in M1 marker, CD86, and shifted to M2 phenotype in HG condition with agm (100  $\mu$ M), indicated by the upregulation of mannose receptor CD206. When agm was treated with HG, the level of LC3-II was increased while p62/SQSTM1 level was downregulated, and the expression of LAMP1 was increased. In transmission electron microscopy, autophagosomes has shown that HG conditions led to severe mitochondrial damage while elongating phagophore membranes and autolysosomes were seen in cells treated with HG and agm, showing stimulated mitophagy. In a high-fat diet-induced T2DM metabolic dementia animal model, agmatine administration upregulated autophagy and shifted microglial polarization from proinflammatory to anti-inflammatory phenotype, improving cognitive function and alleviating neuroinflammation. In this study, it has been demonstrated that agm treatment can ameliorate neuroinflammation by upregulating autophagy on a cellular level and shifting microglia polarization from M1 to M2 phenotype, showing a therapeutic potential in metabolic AD.

**Key words:** Agmatine, High glucose, Microglia, Autophagy, Neuroinflammation

## INTRODUCTION

The neuroinflammatory response following ischemic stroke begins with the activation of innate immune cells to block infection and eliminate pathogens, cell debris, and misfolded proteins [1].

This process subsequently induces the infiltration of adaptive immune cells, leading to irreversible secondary damage [2]. Initially, neuroinflammation plays a role in nerve repair and protection, but excessive activation instigates subsequent damage to neuronal cells, and ultimately leads to various chronic neurological diseases [1, 3]. Activated microglia are crucial in immune responses and inflammatory conditions in the CNS and neurodegenerative diseases [4]. Microglia are a specialized population of cells in the CNS that act as primary immune cells, functioning similarly to macrophages [5]. Under normal physiological conditions, microglia remain in resting phenotype and are involved in neuronal activities,

Submitted February 27, 2025, Revised March 11, 2025,  
Accepted March 11, 2025

\*To whom correspondence should be addressed.  
TEL: 82-2-2228-1646, FAX: 82-2-365-0700  
e-mail: jelee@yuhs.ac

such as neurogenesis, synaptogenesis and release of neurotrophic factors [6]. When distinct stimuli are present, microglia is often polarized into two major activated subtypes, M1 and M2 [7]. Classic M1 polarization is related to proinflammatory conditions, producing and releasing reactive oxygen species (ROS) and cytokines, such as interleukin 12 (IL-12), tumor necrosis factor- $\alpha$  (TNF- $\alpha$ ), and interleukin 1 $\beta$  (IL-1 $\beta$ ), ultimately, contributing to neurodegeneration. Alternative M2 microglia polarization is known to induce anti-inflammatory responses, while limiting neurotoxic effects [5, 7].

In recent years, studies have reported that agmatine is involved in the regulation of microglia polarization and has known neuroprotective effects [8-10]. Agmatine is the main result of L-arginine decarboxylation, which is derived from arginine decarboxylase (ADC) [8]. Research shows agmatine targeting various psychological disorders related to depression, stress, and addiction by modulating targets, such as neurotransmitters, ion channels, and NMDA receptors [8-14]. Studies also suggest that exogenous administration of agmatine has neuroprotective effects in CNS injury, including neurodegenerative diseases, while being involved in modulating M2 macrophage subdivision [10, 14, 15]. Previous research showed that agmatine ameliorates type II diabetes mellitus (T2DM) - induced Alzheimer's disease (AD) - like alterations through reactivation of blunted insulin signaling [16-18].

Although studies indicate the therapeutic effects of agmatine in metabolic-induced neurodegenerative models, the mechanism behind the amelioration of neuroinflammation have not been proven. Autophagy is a natural degradative pathway to remove damaged components in a cell, such as proteins and organelles. Damage in the autophagy pathway is thought to be one of the major factors that contribute to neurodegeneration. Autophagy can be divided into three different forms: microautophagy, macroautophagy, and chaperonemediated autophagy (CMA). These forms are divided based on the way that the damaged components gets transported to the lysosomes for degradation. The main form of autophagy that is related to neurodegeneration is macroautophagy (referred to as "autophagy") [19]. In autophagy, cellular components that need to be recycled are enclosed by autophagy membranes, also known as phagophores, which expand to form double membraned structures, autophagosomes. Autophagosomes are fused with lysosomes or autophagy vacuoles (AV), containing lysosomal enzymes, and ultimately form autolysosomes, which lead to the degradation of the contents within [19, 20].

Recently, a number of studies have shown that autophagy is inhibited when AV accumulates to a degree similar to lysosomal accumulation impairment in neurons [19]. For example, it has been reported that the AV transport and fusion of autophagosome

and lysosome is impaired in AD, a neurodegenerative condition. The impairment in the transport of autophagosomes along the axons of neurons leads to the accumulation of immature and A $\beta$ -generating vacuoles [21]. As the majority of neurodegenerative diseases, initiated by excessive neuroinflammation, are caused by protein accumulation, increasing the degradation process of these aggregates is essential in novel therapies.

In this regard, there is growing evidence that agmatine can modulate M2 polarization of microglia in neuroinflammation of neurodegenerative diseases, including AD, but the precise mechanism remains unclear. This research aims to investigate the effects of agmatine on the regulation of microglial polarization and autophagy in neuroinflammatory conditions in vivo and in vitro.

## MATERIALS AND METHODS

### *Cell culture and drug treatment*

Immortalized murine microglia cell line, exhibiting both phenotypic and functional properties of reactive microglia, was maintained in RPMI with 10% fetal bovine serum (FBS; Thermo Fisher Scientific, Waltham, Massachusetts, United States) and 100  $\mu$ g/ml penicillin/streptomycin (P-S; Thermo Fisher Scientific, Waltham, Massachusetts, United States). Cells were incubated in 5% CO<sub>2</sub> at 37°C. For high glucose injury, cultures were treated with D-glucose (Sigma-Aldrich, St. Louis, Missouri, United States) for 24 hours (hrs) with 1% FBS and 100  $\mu$ g/ml P-S before sampling. For agmatine treatment group, cultures were treated with agmatine (100 $\mu$ M) for 24 hrs before sampling, considering the concentrations used previous studies [22]. We will experiment for the appropriate glucose concentration for this research.

### *Cell viability (MTT assay)*

BV2 cells were seeded at  $1 \times 10^4$  cells/ml in 24-well plates in order to examine the treatment outcomes. After treatment, cells were rinsed with phosphate-buffered saline (PBS) and medium was replaced with serum-free medium with 3-(4,5-dimethylthiazol-2-yl)-2,5-diphenyltetrazolium bromide (MTT) added to achieve a final concentration of 0.5 mg/ml. After the cells were incubated for 2 hrs, the medium was removed and dimethyl sulfoxide (DMSO) was added in order to solubilize the purple formazan product of the reaction. The supernatant was taken from each well and was analyzed with enzyme-linked immunosorbent assay plate reader at 570 nm. Experiments were repeated at least three times. Cell viability was expressed as a percentage relative to the normal control group value, which was considered 100%.

### Cell sampling

BV2 cells were washed three times with ice-cold PBS and collected. Cell pellets were lysed using ice-cold RIPA buffer (Sigma-Aldrich, St. Louis, Missouri, United States). The lysates were centrifuged at 16,000 g for 30 minutes at 4°C in order to generate whole-cell extracts.

### Preparation of A $\beta$ fibrils

A $\beta$ <sub>1-42</sub> was prepared as described previously [23]. In short, A $\beta$ <sub>1-42</sub> peptide (Bachem, Bubendorf, Switzerland) was dissolved to a final concentration of 1 mM in 1,1,1,3,3,3-hexafluoro-2-propanol (HFIP; Sigma-Aldrich, St. Louis, MO, United States). The peptide solutions were divided into 50  $\mu$ l aliquots and the 1,1,1,3,3,3-hexafluoro-2-propanol was eliminated by evaporation under vacuum (SpeedVac Concentrator; Savant Instruments, Hyderabad, India). The dry peptide aliquots were stored at -80°C until use. In order to make fibrillary A $\beta$ <sub>1-42</sub>, A $\beta$ <sub>1-42</sub> was dissolved in anhydrous dimethyl sulfoxide (DMSO, Sigma-Aldrich, St. Louis, MO, United States) to 1 mM and added to conditioning medium (RPMI with 1% FBS) in order to bring the peptides to 100  $\mu$ M. The solution was incubated at 37°C for 24 h.

### Western blotting

Whole brain tissue samples were retrieved through cardiac reperfusion with saline. Tissue was homogenized in lysis buffer and the supernatant was used to calculate the protein concentration with the BCA assay kit (Thermo Fisher Scientific, Waltham, Massachusetts, United States). Ten  $\mu$ l of protein was separated on 10% SDS-PAGE gels and transferred to polyvinylidene difluoride membrane. After blocking the membrane with 5% bovine serum albumin (BSA), the membranes were incubated with primary antibodies, such as recombinant anti-LC3B protein (Abcam, Cambridge, Massachusetts, USA) at 4°C overnight. After washing the membranes with tween-TBS (0.5%) three times, the membranes were incubated in secondary antibodies, such as Alexa Fluor 594 anti-Mouse IgG (Invitrogen, Waltham, Massachusetts, USA) for 2 hrs at room temperature. After washing the membranes with tween-TBS (0.5%) three times, the protein bands were visualized with enhanced chemiluminescence (ECL) reagents. The images were then captured by chemi-luminescent image analyser (LAS 4000, Fujifilm, Tokyo, Japan). The grayscale value of each protein band was analyzed using ImageJ software (Bethesda, Maryland, United States).

### IHC/ICC/immunogold labeling

Samples were washed with iced PBS three times and fixed with 4% paraformaldehyde (PFA). Cells were permeabilized with PBS

in 0.025% Triton X-100 and blocked with BSA-PBS in room temperature (RT). Samples are incubated with primary antibodies, such as recombinant anti-LC3B antibody (Abcam, Cambridge, Massachusetts, USA) overnight in 4°C. Samples were washed with tween-TBS (0.5%) three times. Samples were incubated in secondary antibodies, such as goat anti-rabbit IgG (H+L) Rhodamine (Millipore, St. Louis, Missouri, United States), for 2 hours in RT. Samples were washed with tween-TBS (0.5%) three times and counterstained with DAPI (Invitrogen, Waltham, Massachusetts, United States) for 1 min in RT. Sample images were taken using Zeiss LSM 700 confocal microscope (Carl Zeiss, Thornwood, NY, USA).

### TEM

Samples were fixed for 12 hrs in 2% glutaraldehyde-2% PFA in 0.1M phosphate buffer (PB) and washed in 0.1M PB. Specimens were post-fixed with 1% OSO<sub>4</sub> dissolved in 0.1M PB for 2 hrs and dehydrated with an ascending ethanol series (50%~100%) for 10 minutes each. They were then infiltrated with propylene oxide for 10 minutes. Samples were embedded using Poly/Bed 812 kit (Polysciences) and polymerized in an electron microscope oven (TD-700, DOSAKA, Japan) at 65°C for 12 hrs. The block is equipped with a diamond knife in the Ultramicrotome and is cut into 200 nm semi-thin. For observation through optical microscope, the sections are stained with toluidine blue. The region of interest was cut into 80 nm thin sections using the ultramicrotome, placed on copper grids, double stained with 3% uranyl acetate for 30 minutes and 3% lead citrate for 7 minute staining. The sections were imaged with a transmission electron microscopy (JEM-1011, JEOL, Tokyo, Japan) at the acceleration voltage of 80 kV equipped with a Megaview III CCD camera (Soft-imaging system-Germany). Negative staining was conducted by placing the Formvar-carbon coated EM grid on top of the sample drop for 15 seconds. The grid was removed, blotted with filter paper, and placed on top of a drop of 1% uranyl acetate was placed for 15 seconds. Excess liquid was removed with filter paper and washed with a drop of distilled water. Dried EM grids were observed with transmission electron microscopy (JEM-1011, JEOL).

### Animal procedure

Eight weeks old C57/BL6 (SLC, Shizuoka, Japan) were used in this study. Mice were raised in standard laboratory animal facility under a 12 h light/dark cycle and had access to food and water *ad libitum*. All procedures were conducted in accordance with the National Institutes of Health guidelines for the Care and Use of Laboratory Animals and Yonsei University, College of Medicine, Animal Care and Use committee. Previously established methods

were modified to develop a T2DM mouse model with AD-like alterations [16, 24]. After a week of acclimatization to the laboratory conditions, mice were randomly divided into two groups. Mice were administered either normal chow diet (NC 13.1% kcal fat) or high-fat diet (HFD; 60% kcal fat) for 12 weeks. HFD fed mice were injected interperitoneally with a low dose of streptozotocin (STZ; 100 mg/kg/ip, dissolved in citrate buffer [pH 4.4]) at week 4 in order to shorten the time in establishing the animal model by inducing partial insulin deficiency. Mouse with fasting serum glucose level >370 mg/dl, body weight >40 g and impaired glucose, insulin tolerance was classified as T2DM. T2DM mice were divided into two groups: HFD mice and HFD mice treated with agmatine (HFD+AGM; 100 mg/kg/ip, dissolved in saline). These groups were treated with their according treatments daily for 2 weeks. Six mice were included in each group.

#### ***Determination of body weight and serum glucose levels***

Body weight (BW) and fasting serum glucose levels were monitored biweekly. To measure fasting glucose levels, mice were fasted for 4 hrs before the test. Blood glucose concentrations from blood samples were taken from the tip of the tail and were measured using a glucometer.

#### ***Behavior tests***

##### **Novel object recognition test**

Novel object recognition test (NOR) was conducted over 3 consecutive days: habituation, training, and testing day as previously described [25]. Two easily differentiable objects were chosen for this experiment. Mouse were placed in a square, nonporous plastic chamber. For habituation, mice were individually placed in an empty chamber to freely explore for 5 minutes. For training, two identical objects were placed near the corners of the chamber, positioned diagonally from each other. Each mouse was given 10 minutes in the chamber. For testing, one object, familiar from training, and a novel object were placed in the same manner as habituation testing. Each mouse was given 10 minutes in the chamber to explore. The objects and chambers were thoroughly cleaned with 70% ethanol between each use in order to remove odor cues. The discrimination index was calculated with the data from testing.

##### **Spontaneous alternation Y-maze test**

Spontaneous alternation Y-maze test was tested as previously described [26]. Mice were placed individually in the center of the maze and was given 8 minutes to explore freely. The number of arm entries and the sequence were recorded. Percentage alternation was calculated as followed: number of alternations/number of

possible triads \*100.

#### ***Tissue sample preparation***

Mice were perfused transcardially with saline. Whole brain samples were collected and dissected at the cortex and hippocampus. Samples were frozen in liquid nitrogen and stored at -80°C until further use.

#### ***Statistical analysis***

All data analyses were performed using Prism 9 software (San Diego, California, USA). Data was expressed as standard errors and means (S.E.M.). The significance between the group has been analyzed through one-way ANOVA. Values under 0.05 were considered statistically significant.

## **RESULTS**

#### ***Effects of agmatine administration in BV2 microglia under HG conditions***

In order to investigate the cell viability of BV2 microglia under inflammatory conditions, we conducted MTT assay when treated with glucose (Supplemental Fig. 1A). Cell viability was increased and reduced non-significantly by glucose treatment (25, 50, 75, or 100 mM) in dose dependent manner. 100 mM was selected as high-glucose treatment conditions in subsequent experiments in order to mimic chronic neuroinflammatory conditions considering the results of the MTT assay and previous experimental conditions [22]. In addition, MTT assay was conducted to determine whether agmatine directly affects the cell viability (Supplemental Fig. 1B). Cell viability significantly proliferated in HG group treated with agmatine (HG+agm) compared to HG.

#### ***Agmatine administration alleviates HG-induced autophagy inhibition in BV2 cells***

Various studies indicate that autophagy plays a crucial role in neuroinflammation and can induce shift in microglia phenotype [27-29]. However, it is unclear whether agmatine modulates HG induced microglial polarization by regulating autophagy. To examine the effect of agmatine on autophagy, we tested several protein markers related to autophagy, including LC3, p62, and LAMP1 through western blot and ICC (Fig. 1A). HG treatment did not significantly alter the protein expression levels of LC3-II (Fig. 1B) but increased the levels of p62 (Fig. 1C). On the other hand, post-treatment of agmatine in HG group showed a significant increase in LC3-II levels and a decrease in p62 levels (Fig. 1B, C). As an increase in LC3-II can result from autophagy induction or impairment of lysosomal degradation, we examined LAMP1, lyso-



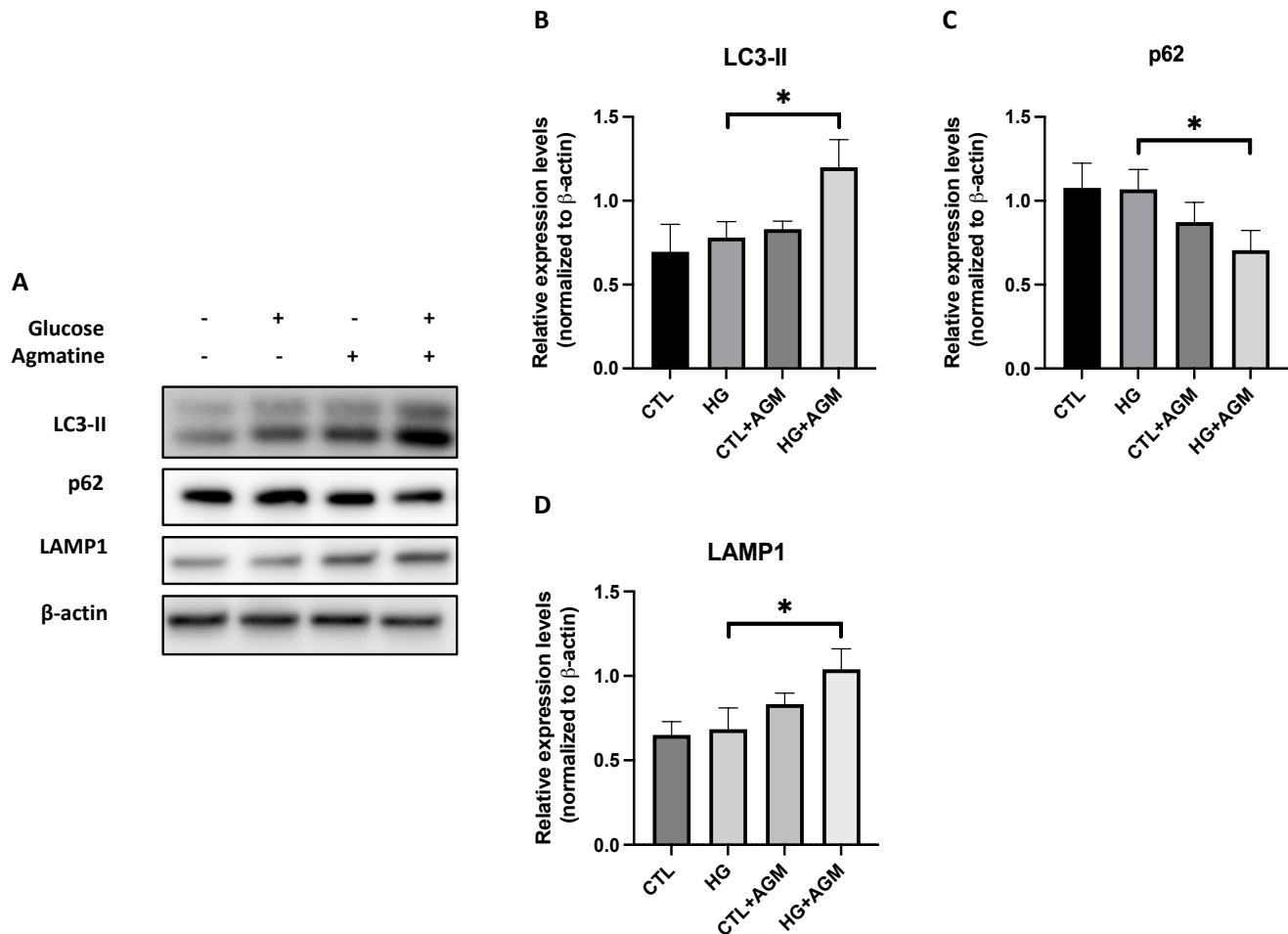


**Fig. 1.** Changes in autophagic flux in HG conditions after agmatine administration. (A) Representative image of the effects of agmatine on protein expression levels of LC3, p62, and LAMP1 by western blot assay. (B) Quantitative analysis of LC3-II relative expression. (C) Quantitative analysis of p62 relative expression. (D) Quantitative analysis of LAMP1. (E) Immunofluorescence staining of LC3 and p62 positive cells. In HG+agm treatment group, not only autophagy process is induced, but augmented as a whole. (F) TEM imaging of BV2 cells before and after drug administration (each group n=4; \*p<0.05; each group n=4; immunofluorescence scale bar=20 μm, TEM scale bar=2,000 and 1,000 nm).

some marker indicating lysosomal compartments. Western blot analysis showed increase in LAMP1 protein levels in HG+agm (Fig. 1D). Increase in colocalization of LC3 and p62 was also seen in HG+agm indicating autophagy (Fig. 1E). Putting these results together, in HG+agm group, autophagic process is not augmented in one certain part, but as a whole.

In addition, we used transmission electron microscopy (TEM) for in situ visualization of the effect that agmatine has on autophagy process. HG injury led to severe mitochondrial damage and shortened membranes. When agmatine was treated to the HG treatment group, elongating phagophore membranes, as well as autolysosomes, the final stage of autophagy that degrades the compartments inside, were observed (Fig. 1F). These results put together show that agmatine induces autophagy in HG conditions.

#### **Agmatine induces M2 microglial polarization under HG-induced inflammatory conditions**

To verify microglia differentiation under HG conditions and agm, western blot and immunocytochemistry were conducted. Proinflammatory M1 polarization marker, CD86, increased significantly under HG compared to control treatment groups and other treatment groups (Fig. 2A~C). LPS was used as a positive control for proinflammatory M1 polarization to compare the expression. Antiinflammatory M2 polarization marker, CD206, was increased significantly in HG+agm, compared to control treatment groups and other treatment groups (Fig. 2A, B, D). IL4 was used as a positive control for anti-inflammatory M2 polarization to compare the expression. On the contrary, the expression of CD206 was dramatically decreased in the HG treatment group (Fig. 2B, D). These results indicate that HG promotes M1 polarization, while

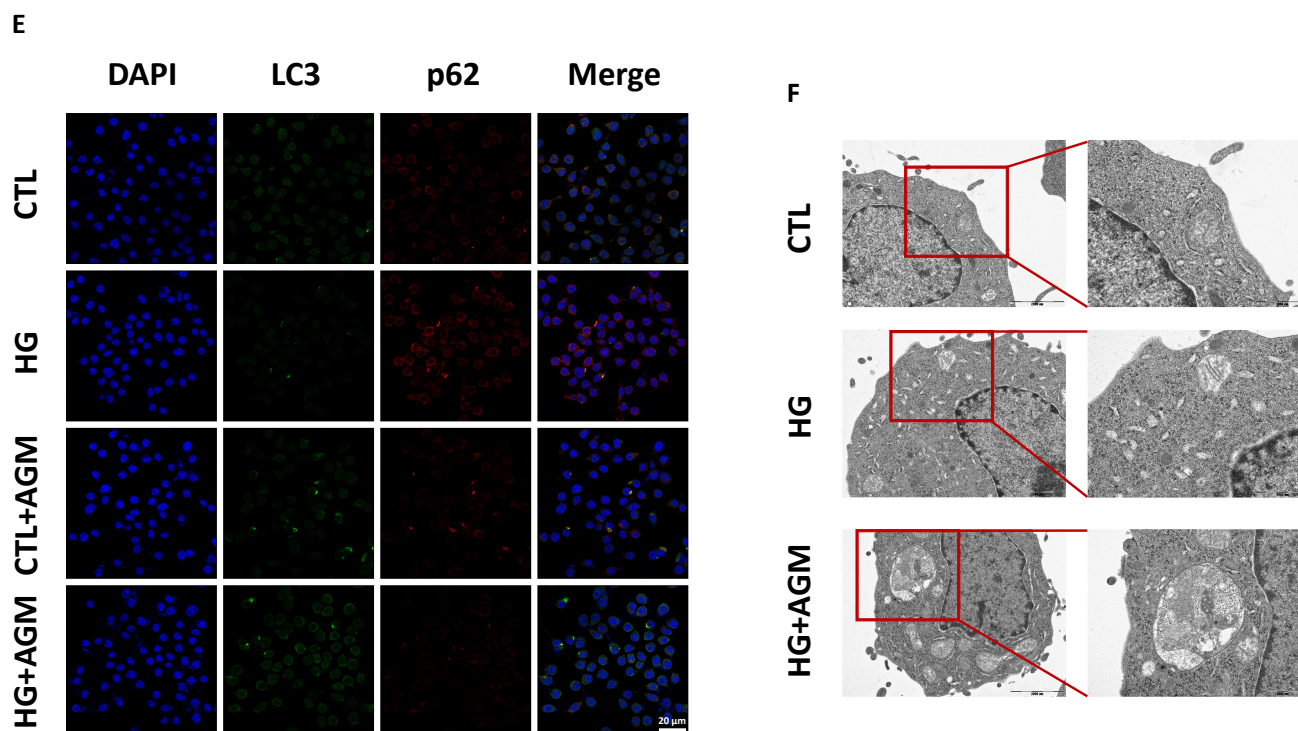


**Fig. 1.** Continued.

agmatine can reverse the inflammatory effect by promoting M1 to M2 polarization in BV2.

#### **Administration of agmatine enhances autophagic clearance of A $\beta$ in BV2 cells treated with fa $\beta$**

To visualize the relationship between autophagic vacuoles and A $\beta$ , treatment of fa $\beta$  was examined. Following the treatment of fa $\beta$ , LC3 puncta increased, indicating autophagy induction by extracellular fa $\beta$ . fa $\beta$  was also internalized and colocalization could be seen within the cells, indicating autophagic clearance of fa $\beta$ . Colocalization of LC3 and fa $\beta$  can also be seen in this group, which indicates autophagic clearance of fa $\beta$  (Fig. 3A). When agmatine is cotreated with fa $\beta$ , LC3 fluorescence puncta increased, indicating agmatine further enhances autophagic induction (Fig. 3B). Autophagic induction was also visualized in TEM imaging. Compared to control groups, when fa $\beta$  was treated, autophagic vacuoles and elongated membranes were seen in various places, indicating induction of autophagy, while fa $\beta$ +agm treatment led to autophagic vacuoles and autophagic degradation, further enhancing the clearance of extracellular debris (Fig. 3C). Furthermore, immunogold staining of fa $\beta$  was conducted to visualize the localization of the extracellular fa $\beta$  within the autophagic structures of the cell. Compared to fa $\beta$  where a few of immunogold specks of fa $\beta$  can be seen within the autophagic organelles, numerous more

immunogold specks can be seen when agmatine was cotreated with fa $\beta$  in the autophagosome, which indicates that agmatine further enhances autophagic clearance of extracellular A $\beta$  (Fig. 3D).

#### **Agmatine induces autophagy and M2 microglial polarization in HFD-induced hyperglycemic mouse model**

As mentioned earlier, previous research indicates that impaired glucose homeostasis, such as type 2 diabetes mellitus (T2DM) and metabolic syndrome, is linked with neurodegenerative diseases [16]. This research is based on the prospect of metabolic dysfunction resulting in the progression of brain damage and cognitive decline, otherwise known as neurodegeneration. Previous research shows the cognitive impairment of high fat diet (HFD)-induced hyperglycemic animal models show that the main cause of AD-like alterations is likely insulin resistance in the brain [16, 17, 30]. As these models are already in use for metabolic dysfunction neurodegenerative animal models, same models have been made according to previous studies (Supplemental Fig. 2A). Eight weeks old C57/BL6 mice were fed 60% high fat diet for 12 weeks. Body weight and fasting glucose levels increased significantly in HFD fed mice compared to ND fed mice (Supplemental Fig. 2B, C). In addition, glucose tolerance and insulin tolerance were significantly altered in HFD fed group compared to ND fed group (Supplemental Fig. 2D, E).

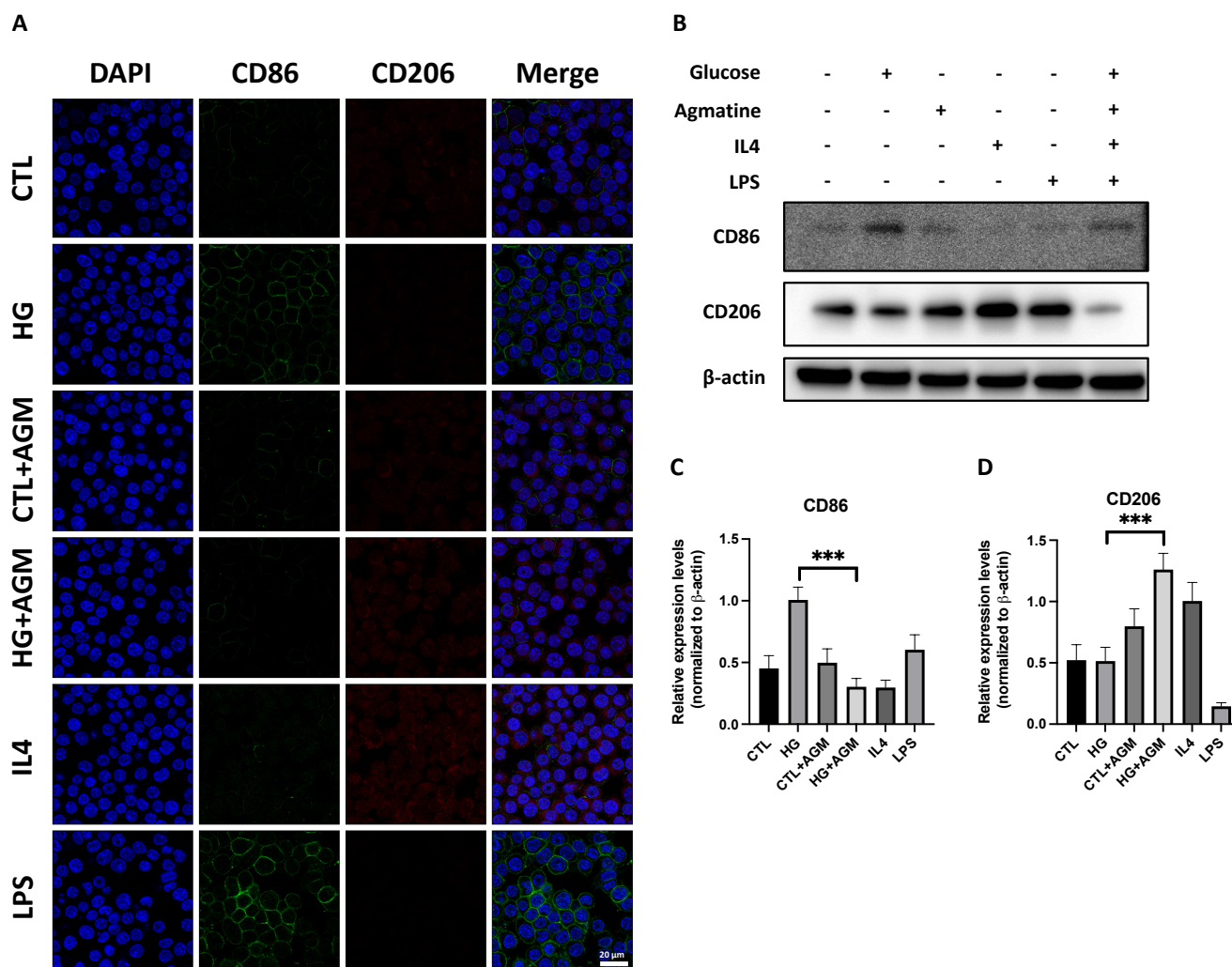


**Fig. 2.** Agmatine administration induces microglial phenotypic shift from M1 to M2 in HG conditions. (A) Immunofluorescence staining of CD86 and CD206 positive cells at 40 $\times$  magnification. (B) Representative image of the effect of agmatine on protein expression levels of CD86 and CD206 by western blot assay. (C) Quantitative analysis of CD86 relative expression. (D) Quantitative analysis of CD206 relative expression (each group n=3; \*\*p<0.01, \*\*\*p<0.001; scale bar=20  $\mu$ m).

Autophagy and microglia activation was tested in HFD induced hyperglycemic dementia animal model when agmatine was administrated. HFD nor administration of agmatine did not significantly alter the expression of LC3-II levels (Fig. 4A, B). On the other hand, with HFD fed mice, the expression of p62 rose significantly, while administration of agmatine significantly decreased the expression level (Fig. 4A, C). Regarding microglia polarization, HFD fed mice had significantly higher expression levels of CD86, proinflammatory microglia, while administration of agmatine to HFD fed mice increased expression of CD206, anti-inflammatory microglia, significantly (Fig. 4D, E).

### Agmatine improves cognitive function in HFD-induced hyperglycemic mice

Behavior tests were conducted to determine whether the M2 phenotypic shift in microglial activation and increase in autophagy will lead to improvement in cognitive function. Novel object recognition test (NOR) was conducted as it is an effective test to test learning and memory in mice while conditions of this test closely resembles the conditions used to study human cognition's spatial memory [31]. This test is based on the natural tendency of mice being attracted towards a novel object. Compared to ND fed mice which have a distinct preference of the new object over the familiar object in exploration time, HFD fed mice do not have a distinct preference between the familiar and novel object (Fig. 5B, C). When HFD fed mice were treated with agmatine, the preference



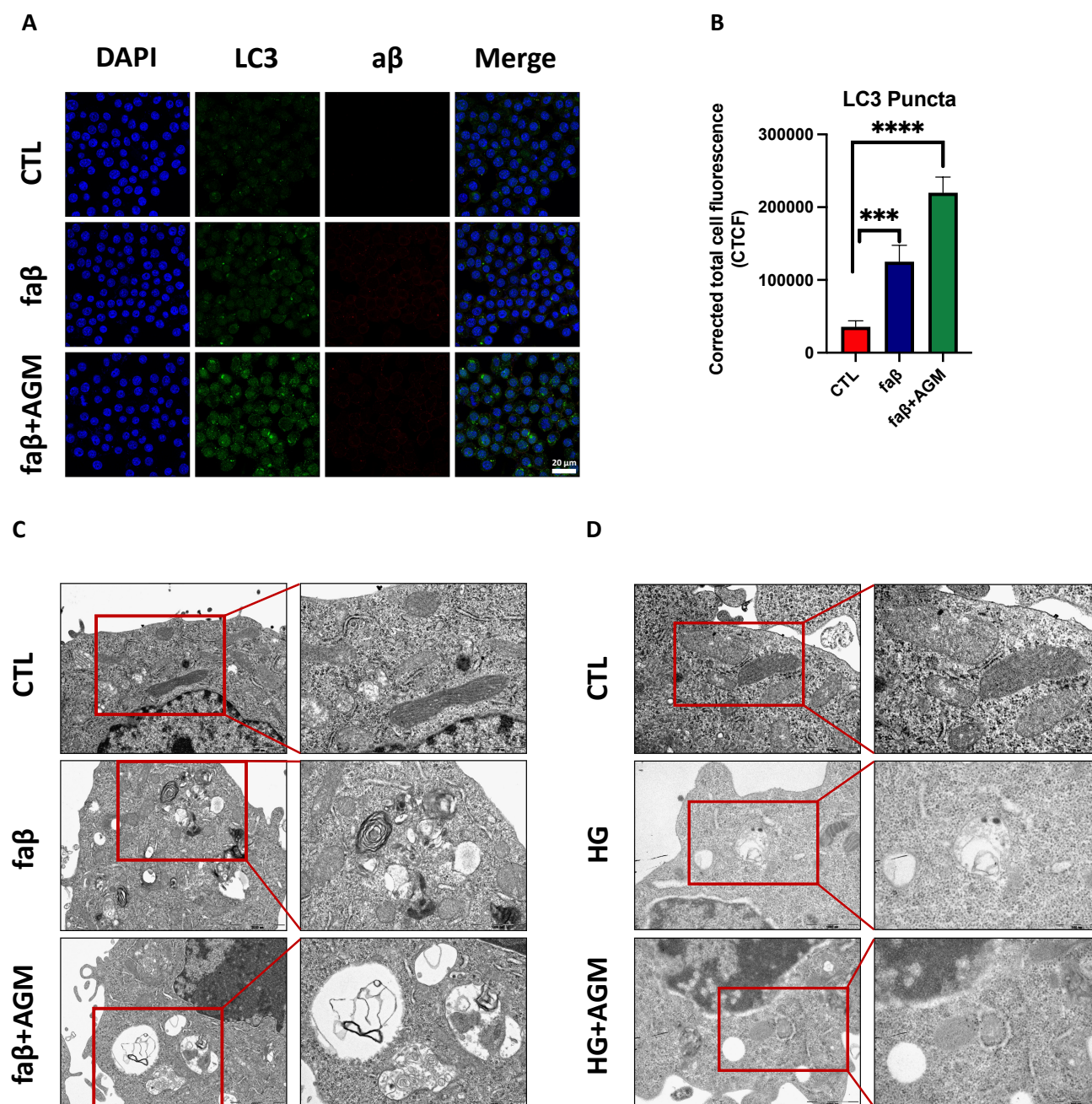


**Fig. 3.** Changes in autophagic flux through faβ and agmatine administration. (A) Immunofluorescence staining of LC3 and faβ positive cells. (B) Quantification of LC3 puncta fluorescence positive cells. (C) TEM imaging of BV2 cells showing autophagic induction treated with faβ. (D) TEM imaging of BV2 cells showing autophagic induction under HG inflammatory conditions (each group n=4; \*\*\*p<0.001, \*\*\*\*p<0.0001; immunofluorescence scale bar represents=20 μm, TEM scale bar=2,000 and 1,000 nm).

between familiar and novel object became more distinct. The significance was seen through the discrimination index comparison (Fig. 5C). HFD fed mice had significantly smaller discrimination index while administration of agmatine significantly increased the percentage.

Furthermore, spontaneous alternation Y-maze test was con-

ducted to assess short term and spatial working memory in mice [32] (Fig. 5D). Higher alternation indicates working short term memory of the animal. HFD fed animal had significantly lower alternation percentage compared to ND fed mice (Fig. 5E). However, agmatine administration led to recovery of alternation percentage. These results indicate that agmatine not only leads to microglial

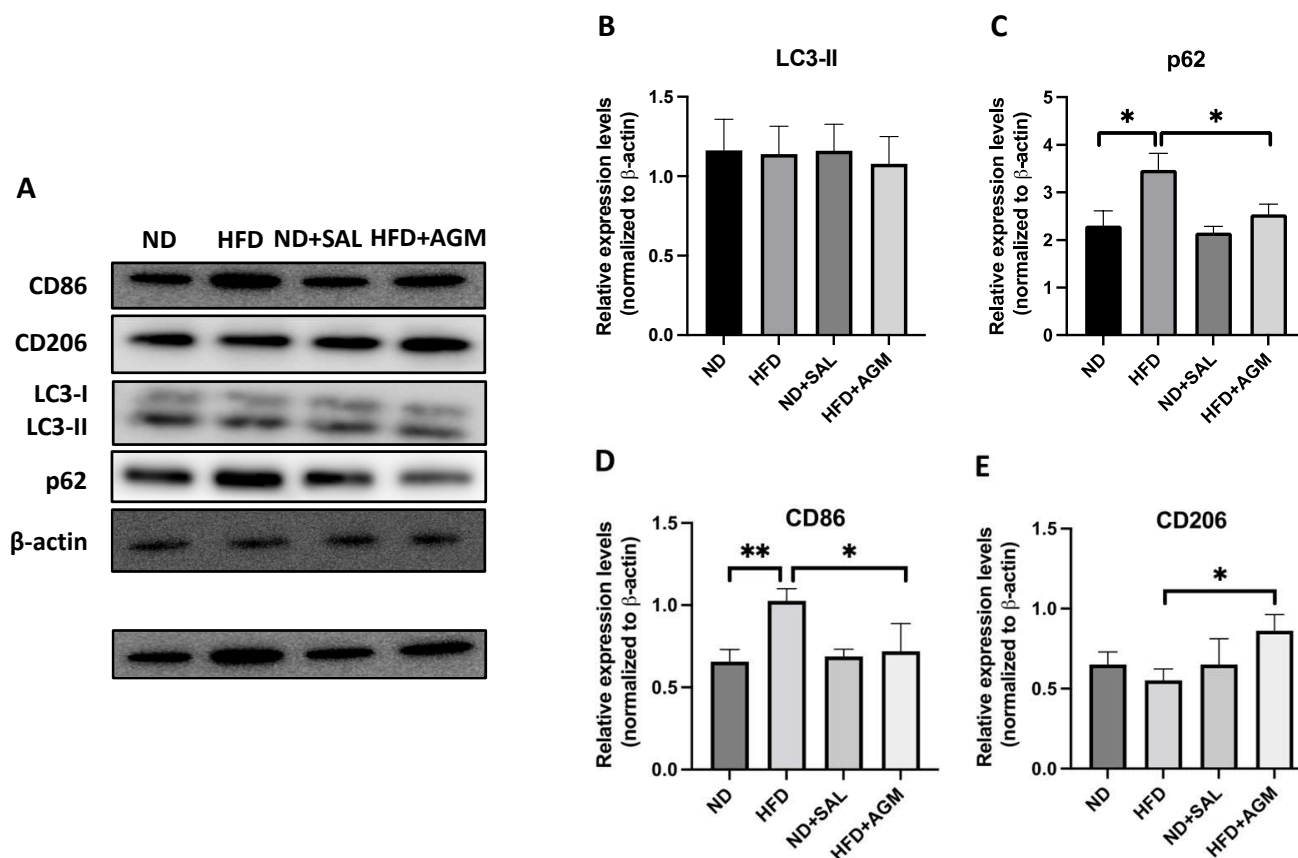


**Fig. 4.** Agmatine administration alters autophagic flux and microglial activation. (A) Representative image of the effect of agmatine on protein expression levels of CD86, CD206, LC3, and p62 by western blot assay. (B) Quantitative analysis of LC3-II relative expression. (C) Quantitative analysis of p62 relative expression. (D) Quantitative analysis of CD86 relative expression. (E) Quantitative analysis of CD206 relative expression (each group n=3; \*p<0.05, \*\*p<0.01).

activation shift and increase in autophagic process, but also ameliorates cognitive function in metabolic neurodegenerative T2DM animal model.

## DISCUSSION

In this study, the effects of agmatine administration have been investigated in neuroinflammatory conditions *in vitro* and *in vivo*, observing the changes in histology as well as cognitive functions. The results of this study has suggested that in neuroinflammatory conditions induced by high glucose injury, agmatine enhances autophagy flux and shifts microglial activation from M1 to M2. Consistent with these observations, it has also been observed that agmatine enhances autophagy when Aβ fibrils were added. The degradation of extracellular Aβ fibrils by autophagic processes were enhanced when agmatine was administered in microglia cell line. These data indicate a novel mechanistic relationship between agmatine and the induction of autophagy, while stimu-

lating phenotypic shift in microglia in inflammatory conditions. Furthermore, in order to investigate the effect of agmatine on ameliorating metabolic neuroinflammatory conditions, agmatine was administered to HFD-induced T2DM-metabolic dementia model. Consistent with the observations *in vitro*, the administration of agmatine increased the autophagic flux in the brain, while shifting microglial activation from proinflammatory M1 to anti-inflammatory M2. In addition, significant improvement in cognitive function was seen in the animal models tested with NOR and spontaneous alternation Y-maze test. Put together, these results indicate the prominent effect of agmatine on ameliorating neuroinflammatory conditions.

Although there is copious research published regarding agmatine and its neuroprotective effects, other studies indicate that agmatine has neuroprotective effects against ischemic/hypoxic, oxygen-glucose deprivation toxicity, traumatic brain injury, spinal cord injury, and more [33-36]. In addition, studies have reported that agmatine is involved in modulating the phenotype of microglia, including



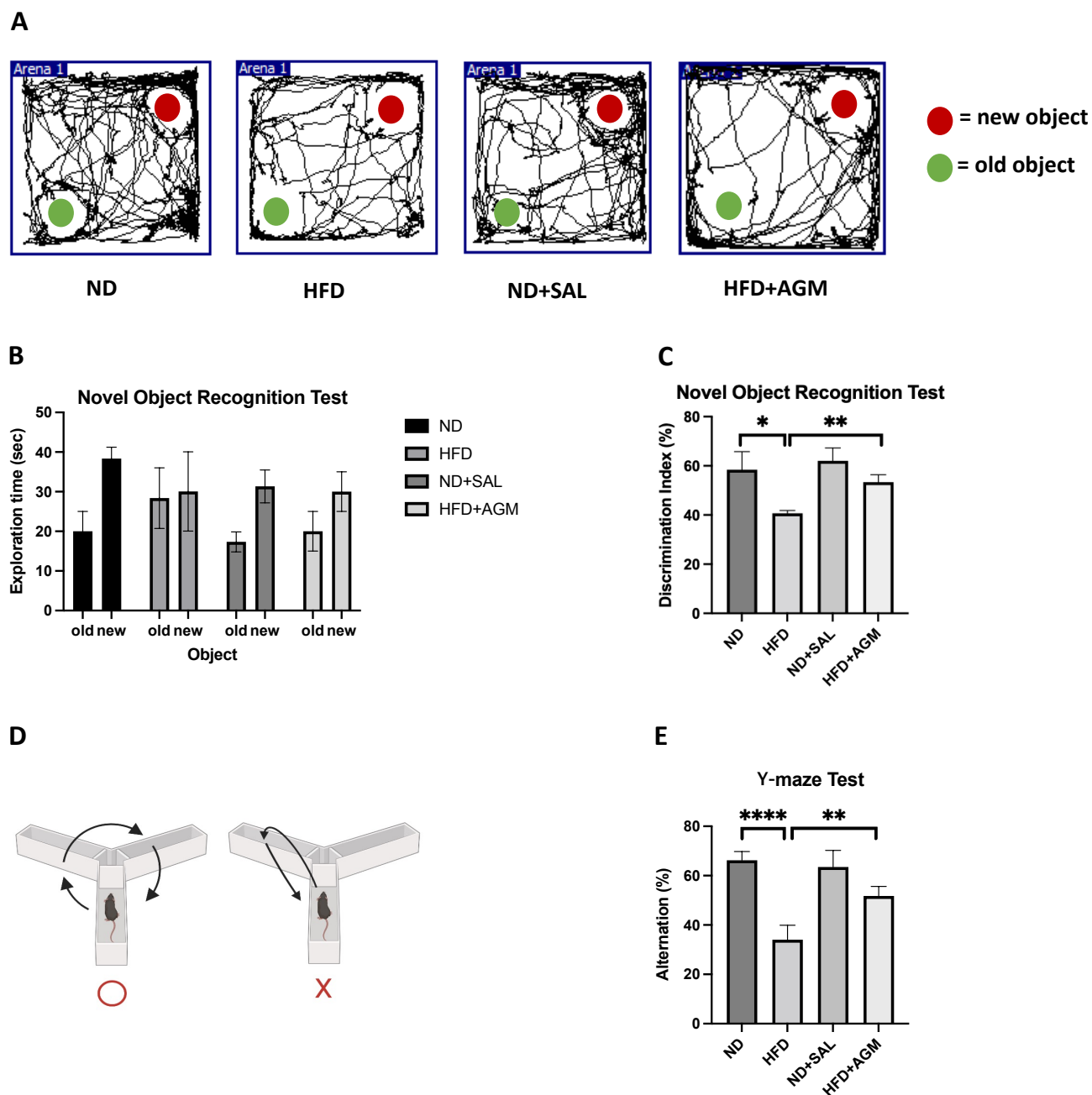


**Fig. 5.** Agmatine enhances memory, cognitive and learning function of HFD-fed mice. (A) NOR travel map of treatment group mice. (B) Preference for old and new object per group in novel object recognition test (NOR). (C) Discrimination index percentage of (NOR). (D) Diagram of Y-maze. (E) Alternation % of Y-maze test (each group n=6; \* $p<0.05$ , \*\* $p<0.01$ , \*\*\*\* $p<0.0001$ ).

a study that agmatine shifts the microglial phenotype from M1 to M2 after acute phase of spinal cord injury in rats [9, 14, 15]. However, this study specifically highlights the ability of agmatine to regulate autophagy and microglial activation in the brain. Numerous studies have reported a link between M2 microglial polarization and an increase in autophagic flux. For example, research has shown that exercise enhances autophagic flux and promotes

the polarization of microglia from the M1 to the M2 phenotype. Additionally, studies indicate that Sestrin2 regulates microglial polarization through mTOR-mediated autophagy in eclampsia. Previous studies indicate exercise or metformin facilitating M1 to M2 microglial polarization by enhancing autophagy through AKT/mTOR pathway [37, 38]. Although there are studies linking anti-inflammatory properties of M2 microglial polarization with

autophagic properties, there are also research linking M1 phenotype with autophagy upregulation. For example, cecal ligation and puncture led to impaired learning and memory, while accumulating LC3-II, decreasing p62, and shifting microglia polarization to M1 phenotype [39]. These findings suggest that autophagy regulation plays a crucial role in the phenotypic transition of microglia.

Modification of neuroinflammation by microglia activation is an important therapeutic target for various neurological diseases including neurodegenerative diseases such as AD and Parkinson's disease (PD). AD is characterized by intraneuronal neurofibrillary tangles (NFTs), comprised of highly phosphorylated forms of tau proteins, and extracellular amyloid plaques, which are consisted of amyloid-beta peptides [40]. However, with the recent increase in obesity rates leading to an increase in type 2 diabetes [41], so many studies have linked this metabolic dysfunction to neurodegenerative diseases such as AD and PD [42-44]. Although there are several drug treatment options available today, such as cholinesterase inhibitors and memantine, which reduce the cognitive symptoms that come along with the disease, none are available today that directly control the levels of NFTs. This study suggests the potential repositioning of agmatine, an already available drug, as a novel mechanism that regulates autophagy and microglial phenotypic transition in neuroinflammatory conditions through the upregulation of LC3-II and LAMP-1.

While this study demonstrates the neuroprotective effects of agmatine in modulating microglial polarization and autophagy under neuroinflammatory conditions, it is important to acknowledge that the observed in vivo behavioral recovery may not be solely attributed to microglial modulation. Agmatine has been reported to exert effects on various cell types in the brain, beyond microglia.

A previous study suggests that agmatine can influence neural progenitor cells by regulating IL-1 $\beta$  expression and promoting neuronal differentiation through TLX modulation [45]. This finding indicates that agmatine may contribute to neuroprotection not only by modulating microglial activation but also by directly affecting neuronal development and repair mechanisms. Thus, while our study highlights the role of agmatine in microglial polarization, additional studies are required to investigate its broader effects on other neural cell populations, such as neurons and astrocytes, under neuroinflammatory and metabolic dysfunction conditions. Future research should aim to dissect the interplay between microglia, neurons, and glial cells in the presence of agmatine to provide a more comprehensive understanding of its therapeutic potential. Therefore, further study is needed to discover the detailed systemic mechanism behind the process of agmatine inducing autophagy and phenotypic shift in microglial cells in neuroinflammatory conditions. This mechanism may be a crucial

therapeutic target in decelerating neurodegenerative diseases, such as AD, as it may be a route in degrading tau tangles or A $\beta$ .

In conclusion, agmatine ameliorates type 2 diabetes metabolic dementia animal model through modulating microglial polarization. These results suggest novel therapeutic usage of agmatine in the pharmaceutical and medical field to cure metabolic neurodegenerative conditions.

## ACKNOWLEDGEMENTS

This study was supported by the National Research Foundation of Korea (NRF) grant funded by the Korean government (MSIT) (RS-2023-00241339 to JYK and NRF-2021R1A2C2008034 to JEL).

## REFERENCES

1. Olajide OA, Sarker SD (2020) Alzheimer's disease: natural products as inhibitors of neuroinflammation. *Inflammopharmacology* 28:1439-1455.
2. Chamorro Á, Meisel A, Planas AM, Urra X, van de Beek D, Veltkamp R (2012) The immunology of acute stroke. *Nat Rev Neurol* 8:401-410.
3. Huang Y, Liao Z, Lin X, Wu X, Chen X, Bai X, Zhuang Y, Yang Y, Zhang J (2019) Overexpression of miR-146a might regulate polarization transitions of BV-2 cells induced by high glucose and glucose fluctuations. *Front Endocrinol (Lausanne)* 10:719.
4. Shabab T, Khanabdali R, Moghadamtousi SZ, Kadir HA, Mohan G (2017) Neuroinflammation pathways: a general review. *Int J Neurosci* 127:624-633.
5. Bachiller S, Jiménez-Ferrer I, Paulus A, Yang Y, Swanberg M, Deierborg T, Boza-Serrano A (2018) Microglia in neurological diseases: a road map to brain-disease dependent-inflammatory response. *Front Cell Neurosci* 12:488.
6. Zhang L, Zhang J, You Z (2018) Switching of the microglial activation phenotype is a possible treatment for depression disorder. *Front Cell Neurosci* 12:306.
7. Jin MM, Wang F, Qi D, Liu WW, Gu C, Mao CJ, Yang YP, Zhao Z, Hu LF, Liu CF (2018) A critical role of autophagy in regulating microglia polarization in neurodegeneration. *Front Aging Neurosci* 10:378.
8. Kosonen R, Barua S, Kim JY, Lee JE (2021) Role of agmatine in the application of neural progenitor cell in central nervous system diseases: therapeutic potentials and effects. *Anat Cell Biol* 54:143-151.
9. Kim JY, Park J, Chang JY, Kim SH, Lee JE (2016) Inflamma-

- tion after ischemic stroke: the role of leukocytes and glial cells. *Exp Neurobiol* 25:241-251.
10. Xu W, Gao L, Li T, Shao A, Zhang J (2018) Neuroprotective role of agmatine in neurological diseases. *Curr Neuropharmacol* 16:1296-1305.
  11. Piletz JE, Aricioglu F, Cheng JT, Fairbanks CA, Gilad VH, Haenisch B, Halaris A, Hong S, Lee JE, Li J, Liu P, Molderings GJ, Rodrigues AL, Satriano J, Seong GJ, Wilcox G, Wu N, Gilad GM (2013) Agmatine: clinical applications after 100 years in translation. *Drug Discov Today* 18:880-893.
  12. Li YF, Chen HX, Liu Y, Zhang YZ, Liu YQ, Li J (2006) Agmatine increases proliferation of cultured hippocampal progenitor cells and hippocampal neurogenesis in chronically stressed mice. *Acta Pharmacol Sin* 27:1395-1400.
  13. Watts D, Pfaffenseller B, Wollenhaupt-Aguiar B, Paul Géa L, Cardoso TA, Kapczinski F (2019) Agmatine as a potential therapeutic intervention in bipolar depression: the preclinical landscape. *Expert Opin Ther Targets* 23:327-339.
  14. Kim JH, Kim JY, Mun CH, Suh M, Lee JE (2017) Agmatine modulates the phenotype of macrophage acute phase after spinal cord injury in rats. *Exp Neurobiol* 26:278-286.
  15. Kim J, Sim AY, Barua S, Kim JY, Lee JE (2023) Agmatine-IRF2BP2 interaction induces M2 phenotype of microglia by increasing IRF2-KLF4 signaling. *Inflamm Res* 72:1203-1213.
  16. Kang S, Kim CH, Jung H, Kim E, Song HT, Lee JE (2017) Agmatine ameliorates type 2 diabetes induced-Alzheimer's disease-like alterations in high-fat diet-fed mice via reactivation of blunted insulin signalling. *Neuropharmacology* 113:467-479.
  17. Lee S, Kim JY, Kim E, Seo K, Kang YJ, Kim JY, Kim CH, Song HT, Saksida LM, Lee JE (2018) Assessment of cognitive impairment in a mouse model of high-fat diet-induced metabolic stress with touchscreen-based automated battery system. *Exp Neurobiol* 27:277-286.
  18. Choi YS, Song JE, Lee JE, Kim E, Kim CH, Kim DH, Song HT (2019) Hyperpolarized [1-13C]lactate flux increased in the hippocampal region in diabetic mice. *Mol Brain* 12:88.
  19. Eshraghi M, Adlimoghaddam A, Mahmoodzadeh A, Sharifzad F, Yasavoli-Sharahi H, Lorzadeh S, Albensi BC, Ghavami S (2021) Alzheimer's disease pathogenesis: role of autophagy and mitophagy focusing in microglia. *Int J Mol Sci* 22:3330.
  20. Yoshii SR, Mizushima N (2017) Monitoring and measuring autophagy. *Int J Mol Sci* 18:1865.
  21. Nah J, Yuan J, Jung YK (2015) Autophagy in neurodegenerative diseases: from mechanism to therapeutic approach. *Mol Cells* 38:381-389.
  22. Song J, Lee JE (2015) ASK1 modulates the expression of microRNA Let7A in microglia under high glucose in vitro condition. *Front Cell Neurosci* 9:198.
  23. Son SM, Jung ES, Shin HJ, Byun J, Mook-Jung I (2012) A $\beta$ -induced formation of autophagosomes is mediated by RAGE-CaMKK $\beta$ -AMPK signaling. *Neurobiol Aging* 33:1006.e11-e23.
  24. Byrne FM, Cheetham S, Vickers S, Chapman V (2015) Characterisation of pain responses in the high fat diet/streptozotocin model of diabetes and the analgesic effects of antidiabetic treatments. *J Diabetes Res* 2015:752481.
  25. Leger M, Quiedeville A, Bouet V, Haelewyn B, Boulouard M, Schumann-Bard P, Freret T (2013) Object recognition test in mice. *Nat Protoc* 8:2531-2537.
  26. Ohno M, Chang L, Tseng W, Oakley H, Citron M, Klein WL, Vassar R, Disterhoft JF (2006) Temporal memory deficits in Alzheimer's mouse models: rescue by genetic deletion of BACE1. *Eur J Neurosci* 23:251-260.
  27. Dang R, Yang M, Cui C, Wang C, Zhang W, Geng C, Han W, Jiang P (2021) Activation of angiotensin-converting enzyme 2/angiotensin (1-7)/mas receptor axis triggers autophagy and suppresses microglia proinflammatory polarization via forkhead box class O1 signaling. *Aging Cell* 20:e13480.
  28. Ji J, Xue TF, Guo XD, Yang J, Guo RB, Wang J, Huang JY, Zhao XJ, Sun XL (2018) Antagonizing peroxisome proliferator-activated receptor  $\gamma$  facilitates M1-to-M2 shift of microglia by enhancing autophagy via the LKB1-AMPK signaling pathway. *Aging Cell* 17:e12774.
  29. He T, Li W, Song Y, Li Z, Tang Y, Zhang Z, Yang GY (2020) Sestrin2 regulates microglia polarization through mTOR-mediated autophagic flux to attenuate inflammation during experimental brain ischemia. *J Neuroinflammation* 17:329.
  30. Sim AY, Choi DH, Kim JY, Kim ER, Goh AR, Lee YH, Lee JE (2023) SGLT2 and DPP4 inhibitors improve Alzheimer's disease-like pathology and cognitive function through distinct mechanisms in a T2D-AD mouse model. *Biomed Pharmacother* 168:115755.
  31. Lueptow LM (2017) Novel object recognition test for the investigation of learning and memory in mice. *J Vis Exp* 126:55718.
  32. Kraeuter AK, Guest PC, Saranyai Z (2019) The Y-maze for assessment of spatial working and reference memory in mice. *Methods Mol Biol* 1916:105-111.
  33. Kotagale NR, Taksande BG, Inamdar NN (2019) Neuroprotective offerings by agmatine. *Neurotoxicology* 73:228-245.
  34. Barua S, Kim JY, Kim JY, Kim JH, Lee JE (2019) Therapeutic effect of agmatine on neurological disease: focus on ion channels and receptors. *Neurochem Res* 44:735-750.

35. Barua S, Sim AY, Kim JY, Shin I, Lee JE (2021) Maintenance of the neuroprotective function of the amino group blocked fluorescence-agmatine. *Neurochem Res* 46:1933-1940.
36. Goh AR, Park J, Sim AY, Koo BN, Lee YH, Kim JY, Lee JE (2024) Modulating monocyte-derived macrophage polarization in cerebral ischemic injury with hyperglycemia. *Exp Neurol* 378:114824.
37. Bai J, Geng B, Wang X, Wang S, Yi Q, Tang Y, Xia Y (2022) Exercise facilitates the M1-to-M2 polarization of microglia by enhancing autophagy via the BDNF/AKT/mTOR pathway in neuropathic pain. *Pain Physician* 25:E1137-E1151.
38. Wu YQ, Xiong J, He ZL, Yuan Y, Wang BN, Xu JY, Wu M, Zhang SS, Cai SF, Zhao JX, Xu K, Zhang HY, Xiao J (2022) Metformin promotes microglial cells to facilitate myelin debris clearance and accelerate nerve repairment after spinal cord injury. *Acta Pharmacol Sin* 43:1360-1371.
39. Shen Y, Zhang Y, Du J, Jiang B, Shan T, Li H, Bao H, Si Y (2021) CXCR5 down-regulation alleviates cognitive dysfunction in a mouse model of sepsis-associated encephalopathy: potential role of microglial autophagy and the p38MAPK/NF- $\kappa$ B/STAT3 signaling pathway. *J Neuroinflammation* 18:246.
40. Soria Lopez JA, González HM, Léger GC (2019) Alzheimer's disease. *Handb Clin Neurol* 167:231-255.
41. Dietz WH (2023) The COVID-19 lockdown increased obesity disparities; will the increases in type 2 diabetes continue? *Obesity (Silver Spring)* 31:699-702.
42. Troshneva AY, Ametov AS (2022) Bolezn' Parkinsona i sakharnyi diabet 2-go tipa: svyaz' mekhanizmov patogeneza i obshchie terapevticheskie podkhody [Parkinson's disease and type 2 diabetes mellitus: interrelation of pathogenetic mechanisms and general therapeutic approaches]. *Zh Nevrol Psikiatr Im S S Korsakova* 122:12-18.
43. Hardy J, de Strooper B, Escott-Price V (2022) Diabetes and Alzheimer's disease: shared genetic susceptibility? *Lancet Neurol* 21:962-964.
44. Ashrafian H, Harling L, Darzi A, Athanasiou T (2013) Neurodegenerative disease and obesity: what is the role of weight loss and bariatric interventions? *Metab Brain Dis* 28:341-353.
45. Song J, Kumar BK, Kang S, Park KA, Lee WT, Lee JE (2013) The effect of agmatine on expression of IL-1 $\beta$  and TLX which promotes neuronal differentiation in lipopolysaccharide-treated neural progenitors. *Exp Neurobiol* 22:268-276.